

# Object-Transportation Control of Cooperative AGV Systems Based on Virtual-Passivity Decentralized Control Algorithm

**Jin Ho Suh**

*Department of Electrical Engineering, Dong-A University, National Research Laboratory (NRL),  
840, Hadan2-Dong Saha-gu, Busan 604-714, Korea*

**Young Jin Lee**

*Department of Electrical Instrument and Control, Korea Aviation Polytechnic College,  
438 Egeum-dong, Sachon City, Kyungnam 664-180, Korea*

**Kwon Soon Lee\***

*Department of Electrical Engineering, Dong-A University, National Research Laboratory (NRL),  
840, Hadan2-Dong Saha-gu, Busan 604-714, Korea*

Automatic guided vehicle in the factory has an important role to advance the flexible manufacturing system. In this paper, we propose a novel object-transportation control algorithm of cooperative AGV systems to apply decentralized control to multiple AGV systems. Each AGV system is under nonholonomic constraints and conveys a common object-transportation in a horizontal plain. Moreover it is shown that cooperative robot systems ensure stability and the velocities of augmented systems convergence to a scaled multiple of each desired velocity field for cooperative AGV systems. Finally, the application of proposed virtual passivity-based decentralized control algorithm via system augmentation is applied to trace a circle. Finally, the simulation and experimental results for the object-transportation by two AGV systems illustrates the validity of the proposed virtual-passivity decentralized control algorithm.

**Key Words :** Automatic Guided Vehicle (AGV), Decentralized Control Algorithm, Passivity, Passive Velocity Field Control (PVFC), Wheeled Mobile Robot (WMR), Lyapunov Stability

## 1. Introduction

Automatic guided vehicle (AGV) systems are used in many environments such as factories, ports, hospitals, farms, etc., yet there are still significant difficulties in measuring vehicle attitude and position. A wheeled mobile robot named AGV is an important element to convey work in the present flexible material handling system of

factory automation and robots with the various kinds of payloads are developed. Therefore, we take a great interest in the cooperative object-transportation system by multiple vehicles. Multiple AGV systems with small payloads collectively transport a large/or heavy palletized load. Such the object-transportation can contribute much to the future logistics system in the factory (Hashimoto et al., 1995).

The traditional manipulation task of a mechanical system is traditionally specified by means of a desired timed trajectory in the workspace. The control objective is to track this trajectory at every instant of time. In many contour following applications, the actual timing in the desired trajectory is unimportant compared to the coordination and synchronization requirement

---

\* Corresponding Author,

**E-mail :** kslee@dau.ac.kr

**TEL :** +82-51-200-7739; **FAX :** 82-51-200-7743

Department of Electrical Engineering, Dong-A University, National Research Laboratory (NRL), 840, Hadan2-Dong Saha-gu, Busan 604-714, Korea. (Manuscript **Received** December 28, 2004; **Revised** July 15, 2004)

between the various degrees of freedom (Park et al., 2002).

From the above considerations, a control methodology known as passive velocity field control (PVFC) was recently proposed in some papers for fully actuated mechanical systems (Li and Horowitz, 2001a ; 2001b). The methodology encoded tasks using time invariant desired velocity fields instead of the more traditional method. The formulation of PVFC scheme has two distinct features as follows :

(1) The task is encoded desired behavior of the mechanical system is specified in terms of velocity fields defined on the configuration manifold of the system.

(2) The mechanical system under closed-loop control appears to be an energetically passive system to its physical environments.

Note that the mechanical system is not required to be at a particular position at each time. Instead, the velocity field guides the robot to approach the contour in a well behaved manner. However, the PVFC scheme applied to a single manipulator could not extend to multiple robot systems.

Multiple robotic systems in coordination can execute various tasks which could not be done by a single manipulator such as the handling of a heavy object, etc. Moreover, many control algorithms have been proposed for the coordinated motion control of multiple robot systems. Especially, the cooperative control problem for multiple AGV systems under the dynamical interactions each other have been actively discussed in the area of robot manipulator and multi-fingered robot hand. In recent years, there has also been a growing interest in the area of mobile robots and vehicles (Kosuge and Oosume, 1996).

The typical control algorithms for multiple AGV systems may be i) centralized control algorithm and ii) decentralized control algorithm. Moreover, several decentralized control schemes have been proposed in order to overcome the problems of centralized control scheme, in which each robot system is controlled by its own controller without explicit communication among multiple systems.

In this paper, we propose a novel object-transportation control algorithm of cooperative AGV systems to apply decentralized control to multiple AGV systems. The considered AGV systems are composed of 3-wheeled mobile robot systems whose subsystems are under nonholonomic constraints and which conveys a common object-transportation in a horizontal plain. Moreover it is shown that cooperative robot systems ensure stability and the velocities of augmented systems convergence to a scaled multiple of each desired velocity field for cooperative AGV systems. Finally, the application of proposed virtual passivity-based decentralized control algorithm via system augmentation is applied to trace a circle. Finally, the simulation and experimental results for the object-transportation by two AGV systems illustrates the validity of the proposed virtual-passivity decentralized control algorithm.

## 2. Cooperative AGV Systems

This section shows the kinematics of a 3-wheeled mobile robot (WMR) like the ones that are usually used in industrial environment. The WMR is a wheeled vehicle which is capable of an autonomous motion without external human driver because it is equipped with motors driven by an embarked computer for its motion (D'Andrea-Novel et al., 1991 ; Campion et al., 1996).

### 2.1 A 3-wheeled mobile robot

In this paper, we consider a 3-WMR with two conventional fixed wheels on the same axle and one conventional off-centered orientable wheel as shown in Fig. 1. The two conventional fixed wheels (① and ②) have a fixed orientation while the orientation of wheel ③ is varying.

According to these descriptions, the geometry of the wheels is completely described by the following class ;  $\{r, l, d_i, \alpha_i, \beta_i, \phi_i ; i=1, 2, 3\}$ , the motion of 3-WMR is then completely described by the following vector of the configuration coordinates :

$$q(t) = (x \ y \ \theta \ \beta \ \phi_1 \ \phi_2 \ \phi_3)^T \quad (1)$$

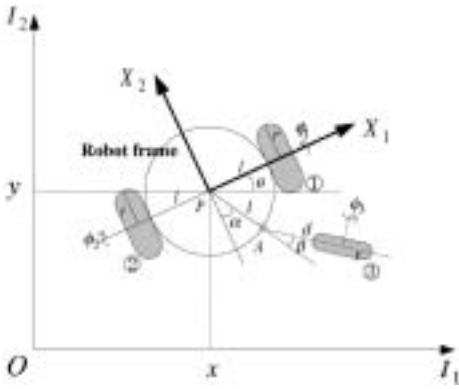


Fig. 1 Configuration of a 3-WMR

The constraint component of this velocity in the plane of the wheel and the component orthogonal to the wheel are defined by the following conditions ; i) along the wheel plane, ii) orthogonal to the wheel plane. With these notations, the kinematical constraints can be calculated as follows :

(1) The pure rolling condition : The component of the velocity of the contact point of the wheel with the ground in the plane of the wheel is zero.

(2) The non-slipping condition : The component of the velocity of the contact point to be orthogonal to the plane of the wheel is zero.

The equation of the posture kinematic model is also described by the compact form as follows :

$$\begin{aligned} \zeta_1(t) &= -\dot{x} \sin \theta + \dot{y} \cos \theta \\ \zeta_2(t) &= \dot{\theta} \end{aligned} \tag{2}$$

Using the Lagrangian formalism for the dynamic equations of a 3-WMR (D’Andrea-Novel, 1991), the dynamic equation can be written and we can represent the following equivalent dynamical state space model :

$$H(\beta) \dot{\zeta}(t) + f(\beta, \zeta) = G(\beta) \tau_m \tag{3}$$

It is easily shown that these constraints are non-holonomic constraints for the system since two vector fields which satisfy the conditions are not involutive (Slotine and Li, 1991).

### 2.2 Cooperative 3-wheeled mobile robots

In this paper, we consider a case where two

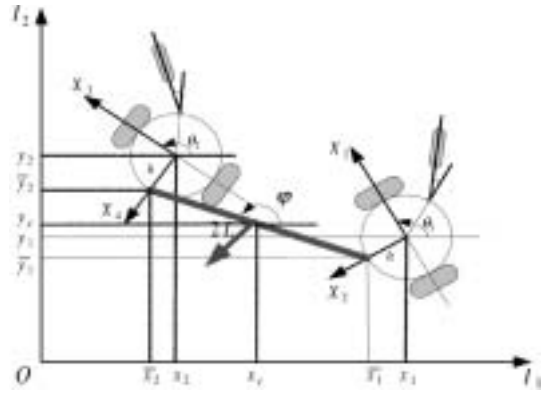


Fig. 2 The configuration of cooperative 3-WMRs

mobile robots convey a rod for simplicity, however, the similar discussion can be applied for cases where more mobile robots is carrying a general planer rigid object. In this section, we consider the configuration of cooperative 3-WMRs as shown in Fig. 2. In considered robot systems, an object denoted by a rod is connected to each mobile robot by a free joint without friction and the length of an object is  $2L$  (Yamakita et al., 1998).

If we assume that mass and inertia of an object are  $m$  and  $I_o$ , and a position of the mass center and rotational angle of an object from  $O-I_1$  in counterclockwise direction are  $(x_c, y_c)$  and  $\varphi$ , then we have free dynamic equations of an object as follows :

$$M_o \ddot{x}_o = 0, I_o \ddot{\varphi} = 0 \tag{4}$$

where

$$M_o = \begin{pmatrix} m & 0 \\ 0 & m \end{pmatrix}, x_o = (x_c \ y_c)^T \tag{5}$$

On the other hand, since the dynamic equation for two 3-WMRs can be described by the previous section which described the modeling of 3-WMR, an augmented dynamic equation is represented as follows :

$$\begin{aligned} & \begin{pmatrix} H_1(\beta_1) & 0 \\ 0 & H_2(\beta_2) \end{pmatrix} \begin{pmatrix} \dot{\eta}_1(t) \\ \dot{\eta}_2(t) \end{pmatrix} + \begin{pmatrix} f_1(\beta_1, \eta_1) \\ f_2(\beta_2, \eta_2) \end{pmatrix} \\ & = \begin{pmatrix} G_1(\beta_1) & 0 \\ 0 & G_2(\beta_2) \end{pmatrix} \begin{pmatrix} \tau_{m1} \\ \tau_{m2} \end{pmatrix} \end{aligned} \tag{6}$$

for simplicity,

$$H^*(\beta) \dot{\eta}(t) + F^*(\beta, \eta) = G^*(\beta) u(t) \tag{7}$$

where  $u(t) = (\tau_{m1} \ \tau_{m2})^T$ ,  $\eta(t) := (\eta_1 \ \eta_2)^T$  to  $\eta_1(t) = (\zeta_1 \ \zeta_2)^T$  and  $\eta_2(t) = (\zeta_3 \ \zeta_4)^T$  for each 3-WMR, and  $\zeta_i(t) \in \mathfrak{R}$ , ( $i=1, 2, 3, 4$ ) is also defined in the previous section, i.e., each subscript number indicates a number of mobile robot except for  $\zeta_i$ . As  $\zeta_i$  disappear alone in the following, we note that there should be no confusion.

On the other hand, using the dynamic equations of an object and each WMR, the whole dynamic system without constraint introduced by passive joints can be represented as follows :

$$\begin{pmatrix} H^*(\beta) & 0_{1 \times 2} & 0 \\ 0_{1 \times 4} & M_o & 0 \\ 0_{1 \times 4} & 0_{1 \times 2} & I_o \end{pmatrix} \begin{pmatrix} \dot{\eta}(t) \\ \dot{x}_o(t) \\ \dot{\varphi}(t) \end{pmatrix} + \begin{pmatrix} F^*(\beta, \eta) \\ 0 \\ 0 \end{pmatrix} = \begin{pmatrix} G^* \\ 0 \\ 0 \end{pmatrix} u(t) \quad (8)$$

This equation is also rewritten by

$$M_w \dot{x}_w + F_w = G_w u \quad (9)$$

From the kinematic constraints by the passive joints, the holonomic constraints between the generalized coordinates are defined by

$$\begin{pmatrix} \bar{x}_1 \\ \bar{y}_2 \end{pmatrix} = \begin{pmatrix} x_1 - h \sin \theta_1 \\ y_1 + h \cos \theta_1 \end{pmatrix} = \begin{pmatrix} x_c - L \cos \varphi \\ y_c + L \sin \varphi \end{pmatrix} \quad (10)$$

$$\begin{pmatrix} \bar{x}_2 \\ \bar{y}_2 \end{pmatrix} = \begin{pmatrix} x_2 - h \sin \theta_2 \\ y_2 + h \cos \theta_2 \end{pmatrix} = \begin{pmatrix} x_c + L \cos \varphi \\ y_c - L \sin \varphi \end{pmatrix} \quad (11)$$

Then, using the differential of Eqs. (10)-(11) and the definition of  $\eta_i(t)$ , we can represent the matrix form as follows :

$$\underbrace{\begin{pmatrix} J_1 & 0_{2 \times 2} \\ & J_o & J_\varphi \\ 0_{2 \times 2} & J_2 & \end{pmatrix}}_{:=J_w} \begin{pmatrix} \eta_1(t) \\ \eta_2(t) \\ \dot{x}_o \\ \dot{\varphi} \end{pmatrix} = \begin{pmatrix} 0_{2 \times 1} \\ 0_{2 \times 1} \\ 0_{2 \times 1} \\ 0 \end{pmatrix}, \text{ i.e., } J_w \dot{x}_w = 0 \quad (12)$$

where

$$J_i = \begin{pmatrix} -\sin \theta_i & -h \cos \theta_i \\ \cos \theta_i & -h \sin \theta_i \end{pmatrix}, \quad (i=1, 2), \quad (13)$$

$$J_o = (-I_{2 \times 2} \ -I_{2 \times 2})^T$$

$$J_\varphi = (-L \sin \varphi \ -L \cos \varphi \ L \sin \varphi \ L \cos \varphi)^T \quad (14)$$

$$x_w = (\eta_1 \ \eta_2 \ \dot{x}_o \ \dot{\varphi})^T \quad (15)$$

Therefore the actual dynamic equation for whole systems in Eq. (9) can be represented as follows :

$$M_w \dot{x}_w + F_w = G_w u - J_w^T \lambda \quad (16)$$

where  $\lambda \in \mathfrak{R}^4$  is a constraint force vector and it is also defined by

$$\lambda = (\lambda_1 \ \lambda_2)^T; \lambda_1 = (\lambda_{m1} \ \lambda_{m2})^T \text{ and } \lambda_2 = (\lambda_{m3} \ \lambda_{m4})^T \quad (17)$$

If we define the constraint force as above equations, Eqs. (16)-(17), the actual dynamic equation of whole system can be decomposed into the following equations using Eq. (16)

$$H_i(\beta_i) \dot{\eta}(t) + f_i(\beta_i, \eta_i) = G_i(\beta_i) \tau_{mi} - J_i^T \lambda_i \quad (i=1, 2) \quad (18)$$

$$M_o \dot{x}_o = -J_o^T \lambda \quad (19)$$

$$I_o \dot{\varphi} = -J_\varphi^T \lambda \quad (20)$$

### 2.3 Minor loop compensation

Since we assume that the constraint forces,  $\lambda_i$  ( $i=1, 2$ ) in Eq. (17) are observed by each force sensor in our control method, then we can define a local control input,  $\tau_{mi}$  ( $i=1, 2$ ) given by

$$\tau_{mi} = G_i^{-1} (H_i v_i + f_i + J_i^T \lambda_i) - G_i^{-1} H_i J_i^T \lambda_i \quad (i=1, 2) \quad (21)$$

where  $v_i$  ( $i=1, 2$ ) is new input and it will also describe in the next. If we inject new control input  $v_i$  into cooperative 3-wheeled mobile robot systems, then we can define the closed loop system substituting Eq. (19) into Eq. (20)

$$\dot{\eta}_i(t) = v_i(t) - J_i^T \lambda_i \quad (i=1, 2) \quad (22)$$

Recomposing Eq. (19), Eq. (20) and Eq. (22), the actual dynamic equation of whole system is described by the matrix form and this equation is described simply as follows :

$$\bar{M}_w \dot{x}_w = \bar{G}_w v(t) - J_w^T \lambda \quad (23)$$

where

$$\bar{M}_w = \begin{pmatrix} I_{2 \times 2} & & & \\ & I_{2 \times 2} & & \\ & & M_o & \\ & & & I_o \end{pmatrix}, \bar{G}_w = \begin{pmatrix} I_{2 \times 2} & 0_{2 \times 2} \\ 0_{2 \times 2} & I_{2 \times 2} \\ & 0_{2 \times 4} \\ & 0_{1 \times 4} \end{pmatrix} \quad (24)$$

$$v = (v_1 \ v_2 \ 0_{2 \times 1} \ 0)^T \quad (25)$$

We note that the minor loop compensation is not necessary for the design of passive velocity field

control, but the computation for the passive velocity field control would become very complex.

Since the motions of  $x_o$  and  $\varphi$  should be controlled in our control problem and the direct control input for  $\varphi$  does not exist, the distributed control method proposed in our previous research (Yamakita et al., 2000 ; Suh et al., 2004) can not be applied for this paper directly. The dynamic equation is transformed by a coordinate transformation and input change in advance so that the dynamic system of  $\varphi$  disappear in the equation. Therefore the control input for  $\varphi$  is realized as an internal force for the motion of  $x_o$ .

Let's define  $\dot{\tilde{x}}_i$  as follows :

$$\dot{\tilde{x}}_i = J_i \eta_i(t) \quad (i=1, 2) \quad (26)$$

Then, using the new coordinate  $\tilde{x}_i$  in Eq. (26), the actual dynamic equation of 3-WMRs given by Eq. (23) can be rewritten by the following equations

$$J_i^{-1} \ddot{\tilde{x}}_i - J_i^{-1} \dot{J}_i J_i^{-1} \dot{\tilde{x}}_i = v_i - J_i^T \lambda_i \quad (i=1, 2) \quad (27)$$

Therefore the actual dynamic equation of whole system given by Eq. (19), Eq. (20), and Eq. (27) can be represented by matrix form as follows :

$$\begin{aligned} & \begin{pmatrix} J_1^{-1} & & & \\ & J_2^{-1} & & \\ & & M_o & \\ & & & I_o \end{pmatrix} \begin{pmatrix} \ddot{\tilde{x}}_1 \\ \ddot{\tilde{x}}_2 \\ \dot{x}_o \\ \dot{\varphi} \end{pmatrix} + \begin{pmatrix} -J_1^{-1} \dot{J}_1 J_1^{-1} \dot{\tilde{x}}_1 \\ -J_2^{-1} \dot{J}_2 J_2^{-1} \dot{\tilde{x}}_2 \\ 0_{2 \times 1} \\ 0 \end{pmatrix} \\ & = \begin{pmatrix} v_1 \\ v_2 \\ 0_{2 \times 1} \\ 0 \end{pmatrix} - \begin{pmatrix} J_1^T & & & \\ 0_{2 \times 2} & 0_{2 \times 2} & & \\ & J_o^T & J_2^T & \\ & & J_\varphi^T & \end{pmatrix} \begin{pmatrix} \lambda_{m1} \\ \lambda_{m2} \\ \lambda_{m3} \\ \lambda_{m4} \end{pmatrix} \end{aligned} \quad (28)$$

To represent the actual dynamic equation of whole system newly, we first define the matrix  $\bar{J}_w$  as follows :

$$\bar{J}_w := \begin{pmatrix} J_1^{-T} & & & \\ & J_2^{-T} & & \\ & & & I_{2 \times 2} \\ & & & 1 \end{pmatrix} \quad (29)$$

At this time, pre-multiplying a matrix defined by Eq. (29) in Eq. (28), we can describe new dynamic equation of whole system as follows :

$$\begin{aligned} & \begin{pmatrix} J_1^{-T} J_1^{-1} & & & \\ & J_2^{-T} J_2^{-1} & & \\ & & M_o & \\ & & & I_o \end{pmatrix} \begin{pmatrix} \ddot{\tilde{x}}_1 \\ \ddot{\tilde{x}}_2 \\ \dot{x}_o \\ \dot{\varphi} \end{pmatrix} + \begin{pmatrix} -J_1^{-T} J_1^{-1} \dot{J}_1 J_1^{-1} \dot{\tilde{x}}_1 \\ -J_2^{-T} J_2^{-1} \dot{J}_2 J_2^{-1} \dot{\tilde{x}}_2 \\ 0 \\ 0 \end{pmatrix} \\ & = \begin{pmatrix} J_1^{-T} v_1 \\ J_2^{-T} v_2 \\ 0 \\ 0 \end{pmatrix} - \underbrace{\begin{pmatrix} I_{2 \times 2} & & & \\ & I_{2 \times 2} & & \\ -I_{2 \times 2} & -I_{2 \times 2} & & \\ & & J_\varphi & \end{pmatrix}}_{:=J_i^T} \begin{pmatrix} \lambda_{m1} \\ \lambda_{m2} \\ \lambda_{m3} \\ \lambda_{m4} \end{pmatrix} \end{aligned} \quad (30)$$

Moreover, using the generalized coordinates in Eq. (12), we can also derived by

$$J_c \dot{\tilde{x}}_w = 0 \quad (31)$$

where  $\tilde{x}_w = (\tilde{x}_1 \ \tilde{x}_2 \ x_o \ \varphi)^T$ . Furthermore if we define new input  $v_i(t)$  in Eq. (21) as follows :

$$v_i(t) = J_i^{-1}(v_i - \dot{J}_i J_i^{-1} \dot{\tilde{x}}_i) + (J_i^T - J_i^{-1}) \lambda_i \quad (i=1, 2) \quad (32)$$

Then the dynamic equation of whole system, Eq. (28), which is represented by new coordinate  $x_i$  ( $i=1, 2$ ), is simply described by

$$\begin{pmatrix} I_{2 \times 2} & & & \\ & I_{2 \times 2} & & \\ & & M_o & \\ & & & I_o \end{pmatrix} \begin{pmatrix} \ddot{\tilde{x}}_1 \\ \ddot{\tilde{x}}_2 \\ \dot{x}_o \\ \dot{\varphi} \end{pmatrix} = \begin{pmatrix} v_1 \\ v_2 \\ 0_{2 \times 1} \\ 0 \end{pmatrix} - \begin{pmatrix} I_{2 \times 2} & & & \\ & I_{2 \times 2} & & \\ -I_{2 \times 2} & -I_{2 \times 2} & & \\ & & J_\varphi & \end{pmatrix} \begin{pmatrix} \lambda_{m1} \\ \lambda_{m2} \\ \lambda_{m3} \\ \lambda_{m4} \end{pmatrix} \quad (33)$$

where  $v_i$  ( $i=1, 2$ ) is an actual control input. Finally, the dynamic equations in Eqs. (31) and (33) can be represented as follows :

$$\bar{M}_w \ddot{\tilde{x}}_w = (v_1 \ v_2 \ 0_{2 \times 1} \ 0)^T - J_c^T \lambda \quad (34)$$

$$J_c \dot{\tilde{x}}_w = 0 \quad (35)$$

Using the generalized coordinate to Eqs. (10) - (11) and the differentiation of these equations, we can derive the following equations from the relationship between the position of mass center  $x_o = (x_c \ y_c)^T$  and new coordinate  $\tilde{x}_i$  ( $i=1, 2$ ) as follows :

$$\begin{pmatrix} \dot{x}_c \\ \dot{y}_c \end{pmatrix} = \underbrace{\begin{pmatrix} -\sin \theta_1 & -h \cos \theta_1 \\ \cos \theta_1 & -h \sin \theta_1 \end{pmatrix}}_{:=J_{o1} = \tilde{x}_1} \begin{pmatrix} \zeta_1 \\ \zeta_2 \end{pmatrix} + \underbrace{\begin{pmatrix} -L \sin \varphi \\ -L \cos \varphi \end{pmatrix}}_{:=\{I_{2 \times 2} \ 0_{2 \times 2}\} J_\varphi} \dot{\varphi} \quad (36)$$

$$\begin{pmatrix} \dot{x}_c \\ \dot{y}_c \end{pmatrix} = \underbrace{\begin{pmatrix} -\sin \theta_2 & -h \cos \theta_2 \\ \cos \theta_2 & -h \sin \theta_2 \end{pmatrix}}_{:=J_{o2} = \tilde{x}_2} \begin{pmatrix} \zeta_3 \\ \zeta_4 \end{pmatrix} + \underbrace{\begin{pmatrix} L \sin \varphi \\ L \cos \varphi \end{pmatrix}}_{:=\{0_{2 \times 2} \ I_{2 \times 2}\} J_\varphi} \dot{\varphi} \quad (37)$$

Furthermore, substituting the differentiations of

Eqs. (36)-(37) into Eq. (34), we can also describe as follows :

$$\dot{x}_o - (I_{2 \times 2} \ 0_{2 \times 2}) (J_\varphi \dot{\varphi} + \dot{J}_\varphi \varphi) = v_1 - \lambda_1 \quad (38)$$

$$\dot{x}_o - (0_{2 \times 2} \ I_{2 \times 2}) (J_\varphi \dot{\varphi} + \dot{J}_\varphi \varphi) = v_2 - \lambda_2 \quad (39)$$

### 3. Decentralized PVFC Algorithm

In order to design the decentralized PVFC, we assume that  $\dot{\varphi}$  is measurable for each subsystem in this paper, which is a crucial step to derive the decentralized PVFC since  $\dot{\varphi}$  is determined based on both  $\lambda_1$  and  $\lambda_2$ , and both signals can not be used for each subsystem in the decentralized formulation. However since it is difficult to measure the signal in practice, we will estimate the signal from the angle and angular velocity using observer, respectively. Furthermore, the decentralized PVFC scheme in this paper is shown in Fig. 3.

#### 3.1 Augmented mechanical system

If the actual control input is defined as

$$v_1 = v'_1 - (I_{2 \times 2} \ 0_{2 \times 2}) (J_\varphi \dot{\varphi} + \dot{J}_\varphi \varphi) \quad (40)$$

$$v_2 = v'_2 - (0_{2 \times 2} \ I_{2 \times 2}) (J_\varphi \dot{\varphi} + \dot{J}_\varphi \varphi) \quad (41)$$

Then we can rewrite Eq. (38) and Eq. (39) as follows :

$$\dot{x}_o = v'_i - \lambda_i \quad (i=1, 2) \quad (42)$$

Adding the dynamic equation of  $x_o$  in Eq. (33) and Eq. (42), we can describe the motion equation of an object as follows :

$$(I_{2 \times 2} + M_o + I_{2 \times 2}) \dot{x}_o = v'_1 + v'_2 \quad (43)$$

In Eq. (43), it can be seen that the dynamic equation of mass center  $x_o$  is the same as that of connected three masses  $I_{2 \times 2}$ ,  $M_o$ , and  $I_{2 \times 2}$ , and the separated masses are controlled by  $v'_1$  and  $v'_2$ , respectively.

Therefore we can apply a decentralized PVFC proposed in our previous researches to design  $v'_i$  ( $i=1, 2$ ) (Yamakita, 1998 and 2000).

First of all, the procedure in order to apply an individual PVFC algorithm can be designed that the motion equation in Eq. (43) is separated as the following virtual dynamic equation

$$(I_{2 \times 2} + \rho_1 M_o) \dot{x}_o = v'_1 \quad (44)$$

$$(I_{2 \times 2} + \rho_2 M_o) \dot{x}_o = v'_2 \quad (45)$$

for simplicity,

$$\bar{M}'_i \dot{x}_o = v'_i \quad (i=1, 2) \quad (46)$$

where  $\rho_i$  ( $i=1, 2$ ) is load sharing coefficient and it is satisfied with  $\sum_{i=1}^2 \rho_i = 1$ .

Moreover, the dynamics of virtual flywheel is defined as follows :

$$M_{fwi} \dot{x}_{fwi} = v_{fwi} \quad (i=1, 2) \quad (47)$$

where  $v_{fwi}$  ( $i=1, 2$ ) is the coupling control input to the flywheel, which will be defined later on. Thus, the dynamics of the augmented system are composed as follows :

$$\begin{pmatrix} \bar{M}'_i & 0 \\ 0 & M_{fwi} \end{pmatrix} \begin{pmatrix} \dot{x}_o \\ \dot{x}_{fwi} \end{pmatrix} = \begin{pmatrix} v'_i \\ v_{fwi} \end{pmatrix}, \text{ i.e., } \bar{M}'_{ai} \dot{X}_{ai} = v'_{ai} \quad (48)$$

( $i=1, 2$ )

where  $\dot{X}_{ai} = (\dot{x}_o \ \dot{x}_{fwi})^T$  is the velocity of the augmented system,  $v'_{ai}$  is the augmented control input.

#### 3.2 Generation of augmented desired velocity field

For the augmented mechanical system, an augmented desired velocity field  $V_{ai}$  is needed. It is defined so that the following condition is satisfied (Yamakita et al., 2000):

**Condition 1:** The augmented desired velocity field  $V_{ai}$  satisfies :

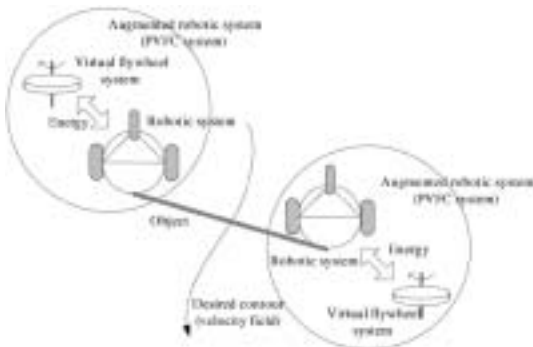


Fig. 3 Schematic diagram of decentralized PVFC algorithm

*Conservation of kinetic energy* : The total kinetic energy of the augmented system  $\bar{H}'_a$  evaluated at the desired velocity field is constant, i.e., the following condition is satisfied for all  $X_{ai}$  :

$$\bar{H}'_{ai} = \sum_{i=1}^2 \frac{1}{2} \dot{X}'_{ai} \bar{M}'_{ai} \dot{X}_{ai} = \bar{E}_i > 0 \quad (49)$$

where  $\bar{E}_i$  is a positive constant.

*Consistency* : The component of the augmented velocity field that corresponds to the original dynamic equation of motion system should be the same as the specified desired velocity field, i.e.,  $V_{ai}$  is of the form :

$$V_{ai} = (V_i \ V_{n+1})^T \quad (50)$$

In this condition 1, it implies that  $V_{ai}$  can be defined by first specifying  $\bar{E}_i$  and then by determining the desired velocity field for the virtual inertia  $V_{n+1}$  in Eq. (50) using

$$V_{n+1} = \sqrt{\frac{2}{M_{fwi}} \left( \bar{E}_i - \frac{1}{2} V_i \bar{M}'_{ai} V_i \right)} \quad (51)$$

Notice that  $\bar{E}_i (i=1, 2)$  should be selected to be large enough so that Eq. (51) has a real solution. It should now be apparent that the virtual inertia acts as a reservoir of kinetic energy.

### 3.3 Coupling control law

As expressed by an original PVFC algorithm, the coupling control law for augmented system is given by

$$v'_{ai} = (\bar{G}_{ai} + \gamma_i \bar{R}_{ai}) \dot{X}_{ai} \quad (i=1, 2) \quad (52)$$

where

$$\bar{G}_{ai} = \frac{1}{2\bar{E}_i} \underbrace{(\bar{\Delta}_{ai} \bar{Q}'_{ai} - \bar{Q}_{ai} \bar{\Delta}'_{ai})}_{skew\ symmetric} \quad (53)$$

$$\bar{R}_{ai} = \underbrace{\bar{Q}_{ai} \bar{P}'_{ai} - \bar{P}_{ai} \bar{Q}'_{ai}}_{skew\ symmetric}$$

$$\begin{aligned} \bar{P}_{ai} &= \bar{M}'_{ai} \dot{X}_{ai} \\ \bar{Q}_{ai} &= \bar{M}'_{ai} V_{ai} \text{ and } \bar{\Delta}_{ai} = \bar{M}'_{ai} \dot{V}_{ai} \end{aligned} \quad (54)$$

where  $\bar{P}_{ai}$ ,  $\bar{Q}_{ai}$ , and  $\bar{\Delta}_{ai} (i=1, 2)$  are the momentums of the augmented system, the desired mo-

mentums of the augmented system, and the momentums of associated with the covariant derivative of the desired velocity field with respect to the actual robot velocities, respectively. And  $\gamma_i (i=1, 2)$  is a control gain, not necessary positive, which determines the convergence rate and the sense in which the desired velocity field will be followed.

For any  $\alpha_i \in \mathfrak{R}$ , the local coordinate representation of the augmented  $\alpha$ -velocity error  $e_{ai}$  is defined by

$$e_{ai} = \dot{X}_{ai} - \alpha_i V_{ai} \quad (55)$$

Thus, using Eqs. (53) - (55) and some algebra, we can obtain the error dynamics for the augmented system in Eq. (48) as follows :

$$\bar{M}'_{ai} \dot{e}_{ai} = \bar{G}_{ai} e_{ai} + \gamma_i \bar{R}_{ai} \dot{X}_{ai} \quad (56)$$

**Theorem 1** : Consider the feedback system for decentralized PVFC as shown in Fig. 5 where the motion equation is given by Eq. (46), and the individual PVFC control law consists of the virtual dynamic augmentation Eq. (47) and coupling control law Eqs. (52) - (54). Furthermore if the control input about control internal force is defined by

$$v'_{ii} = (1 + k_f) \begin{pmatrix} F_{ai} \\ 0 \end{pmatrix} \quad (57)$$

and an actual control input about given system  $v'_i$  is also defined by

$$v'_i = v'_{ai} + v'_{ii} \quad (58)$$

where  $v'_{ii}$  is desired internal force and satisfies  $\sum_{i=1}^2 v'_{ii} = 0$ . Then the passivity and convergence properties of decentralized PVFC are summarized as follows :

(1) The augmented feedback system in Eq. (48) is passive with respect to the supply rate defined by :

$$s(F, \dot{x}) = \langle F, \dot{x} \rangle = F^T \dot{x} \quad (59)$$

where  $F$  and  $\dot{x}$  are input and output, respectively.

(2) For the augmented  $\alpha_i$ -velocity error  $e_{ai}$  in Eq. (55), the velocity of an object  $\dot{X}_{ai}$  is a Lyapunov stable solution in the absence of environment forces.

*Proof of (1)* : The derivation of kinetic energy defined by Eq. (49) satisfies

$$\begin{aligned} \frac{d}{dt} \bar{H}'_{ai} &= \sum_{i=1}^2 \left( \dot{X}'_{ai} \bar{M}'_{ai} \ddot{X}_{ai} + \frac{1}{2} \dot{X}'_{ai} \bar{M}'_{ai} \dot{X}_{ai} \right) \\ &= \sum_{i=1}^2 (\dot{x}'_o \bar{M}'_i \ddot{x}_o + \dot{x}'_{fwi} \underbrace{\bar{M}'_{fwi} \dot{x}'_{fwi}}_{=v_{fwi}}) + \frac{1}{2} \sum_{i=1}^2 \underbrace{\dot{X}'_{ai} \bar{M}'_{ai} \dot{X}_{ai}}_{=0} \quad (60) \\ &= \dot{x}'_o \sum_{i=1}^2 v'_i + \sum_{i=1}^2 \dot{x}'_{fwi} v_{fwi} = \sum_{i=1}^2 \dot{X}'_{ai} v'_{ai} = 0 \end{aligned}$$

Therefore, upon integration of Eq. (60), we can obtain

$$\begin{aligned} \int_0^T \dot{H}'_{ai}(t) dt &= \bar{H}_a(t) - \bar{H}_a(0) \quad (61) \\ &= 0 > -\bar{H}'_a(0) \end{aligned}$$

Since  $\bar{H}'_a(0) \geq 0$ , the system is passive with respect to the supply rate in Eq. (59).

*Proof of (2)* : Given  $\alpha \in \mathfrak{R}$ , let's define the positive definite storage function  $\bar{W}_\alpha$  as follows :

$$\bar{W}_\alpha = \frac{1}{2} \sum_{i=1}^2 e_{ai}^T \bar{M}'_{ai} e_{ai} \quad (62)$$

Differentiating Eq. (62), utilizing Eq. (56) and the fact that  $\bar{M}'_{ai} + 2\bar{G}'_{ai}$  is skew symmetric, we obtain

$$\begin{aligned} \frac{d}{dt} \bar{W}_\alpha &= \frac{1}{2} \sum_{i=1}^2 (\dot{e}_{ai}^T \bar{M}'_{ai} e_{ai} + \underbrace{e_{ai}^T \bar{M}'_{ai} \dot{e}_{ai}}_{=0} + e_{ai}^T \bar{M}'_{ai} \dot{e}_{ai}) \\ &= -\sum_{i=1}^2 \alpha_i \gamma_i \left\{ \underbrace{V_{ai}^T \bar{M}'_{ai} V_{ai}}_{=2\bar{E}_i} \cdot \underbrace{\dot{X}'_{ai} \bar{M}'_{ai} \dot{X}_{ai}}_{=2\bar{H}'_{ai}} - \underbrace{(V_{ai}^T \bar{M}'_{ai} \dot{X}_{ai})^2}_{=2\langle V_{ai}, \dot{X}_{ai} \rangle_{\alpha_i}} \right\} \quad (63) \\ &= -\sum_{i=1}^2 \alpha_i \gamma_i (4\bar{H}'_{ai} \bar{E}_i - \langle V_{ai}, \dot{X}_{ai} \rangle_{\alpha_i}^2) \leq 0 \end{aligned}$$

Since  $\bar{W}_\alpha$  is a positive definite function of  $\alpha_i$ -velocity error  $e_{ai}$ , we know that the augmented  $\alpha_i$ -velocity error velocity error  $e_{ai} = 0$  is Lyapunov stable of the error dynamics using Barlalet's lemma (Slotine and Li, 1991).

## 4. Numerical Simulation

This section illustrates the performance of the proposed control algorithm for cooperative 3-WMRs using numerical simulations. The considered dynamic models will use the similar ones for the constructed experimental system.

Since the desired velocity field is defined such that if a point moves along the desired velocity, the point converges to a circle whose center and radius are the origin and 1[m] at a constant speed in an anti-clockwise direction. For the control of angle of an object  $\varphi$ , desired angle and angular velocity  $\varphi_d$  and  $\dot{\varphi}_d$  are defined as follows :

$$\varphi_d = -\tan^{-1} \left( \frac{y_c}{x_c} \right), \quad \dot{\varphi}_d = \frac{d}{dt} \varphi_d \Big|_{\substack{\dot{x}_c = \dot{x}_{cd} \\ \dot{y}_c = \dot{y}_{cd}}} \quad (64)$$

where  $\dot{x}_{cd}$  and  $\dot{y}_{cd}$  are the desired velocity specified by a desired velocity field in decentralized PVFC as shown in Fig. 4, respectively. A control input  $v_\varphi$  is determined by

$$v_\varphi = -K_v(\varphi_d - \varphi) - K_p(\dot{\varphi}_d - \dot{\varphi}) \quad (65)$$

and  $v_I$  was set to 0. The control is used for both robots and load sharing parameters  $\rho_i$  is set to 0.5 since we assumed that each mobile robot has the same capability. For the observation of  $\dot{\varphi}$ , we will use a minimal order observer which is designed based on triple integrator model where the pole of the observer was chosen to  $-50$ . The various system parameters and the initial states used in numerical simulations are defined as follows :

$$\bar{E}_i = 5000 [\text{Nm}], \quad L = 0.2 [\text{m}]$$

$$K_v = K_p = 4.0, \quad \gamma = 1.0$$

$$(x_1, y_1) = (x_2, y_2) = (1.0, 1.0)$$

$$\theta_1 = \theta_2 = \pi/2, \quad \varphi = -1.7$$

Moreover, in Eqs. (91)-(92) for the proposed control algorithm, they conclude  $\dot{\varphi}$  which actually is impossible to measure. Therefore we need to use the estimate value of  $\dot{\varphi}$ . Assume that  $\varphi^{(3)} = 0$  and the observer can be represented by Gopinath's design method as follows :

$$\begin{aligned} \dot{\zeta} &= -K_{ob} \zeta - K_{ob}^2 \hat{\varphi} \\ \hat{\varphi} &= \zeta + K_{ob} \varphi \end{aligned} \quad (66)$$

where  $K_{ob}$  is observer gain. When we include the external force (10, 0) [N] to system from  $t = 15$  [sec] to  $t = 20$  [sec], the simulation results for considered system are shown in Figs. 4~7, respectively.



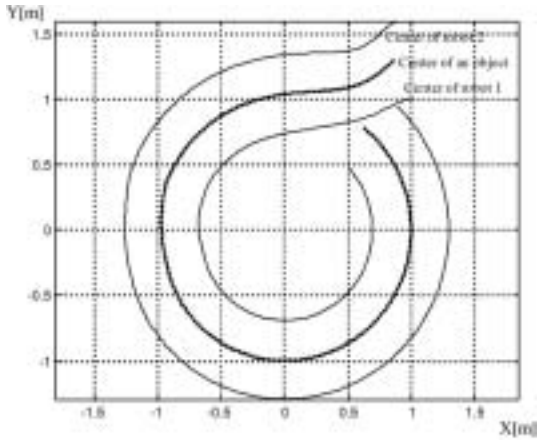


Fig. 4 Trajectories for cooperative 3-wheeled mobile robots and an object

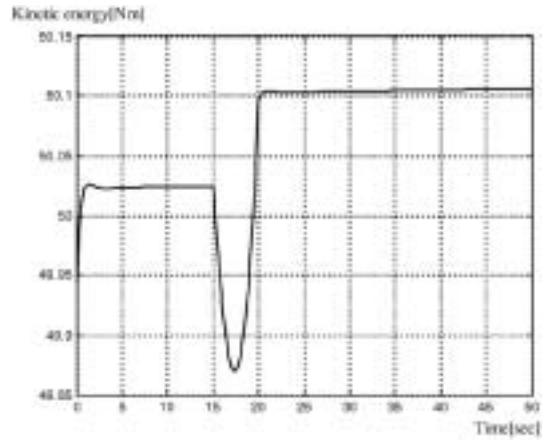


Fig. 7 Kinetic energy of augmented system

### 5. Experimental Results

The constructed experimental system consists of two Nomad Scouts and an object to be a wooden plate as shown in Fig. 8. Moreover the concrete structure of experimental system for cooperative 3-WMRs is shown in Fig. 9.

In the experiment, the control period is set to 2[m·sec] and the constraint force  $\lambda_e$  is also measured through a filter whose transfer function is  $10/(s+1)$  for each subsystem. The position and the orientation of robots are estimated by dead reckoning, and the dynamic parameters of the robot are identified off-line. The desired velocity field is defined such that if a point moves along the desired velocity. Then, the point convergences to a circle whose center and radius are the origin

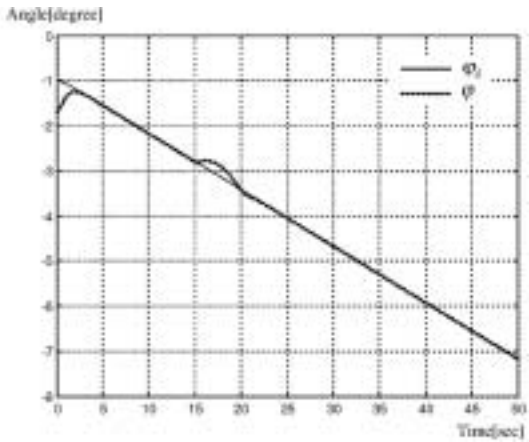


Fig. 5 Tracking angle of an angle and desired angle of an object

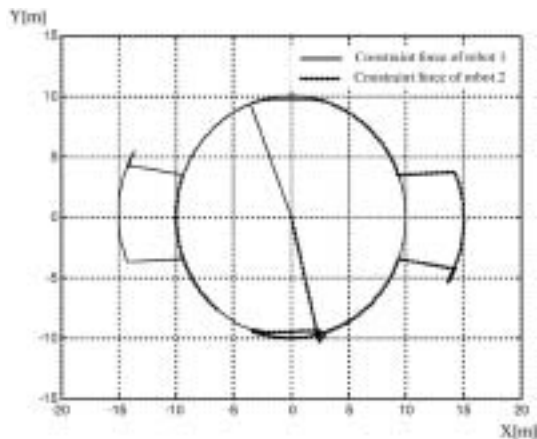


Fig. 6 Constraint forces with disturbance



Fig. 8 Cooperative 3-WMR Systems

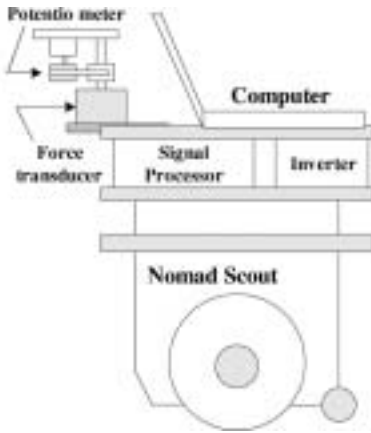


Fig. 9 An outline of experimental system

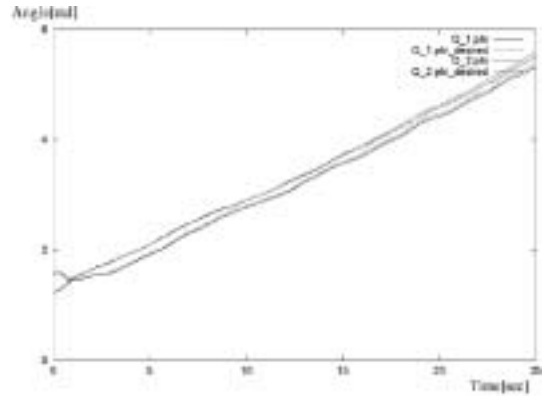


Fig. 11 Tracking angle of an angle and desired angle of an object

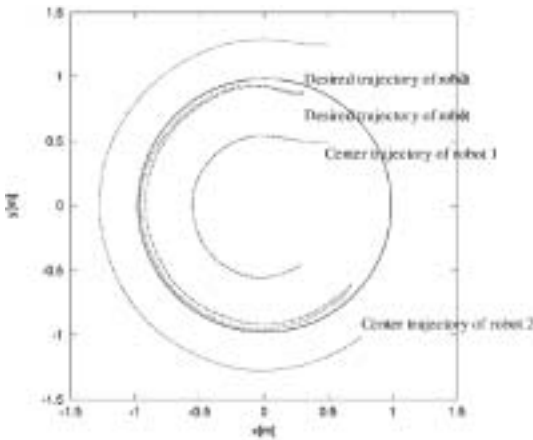


Fig. 10 Trajectories for cooperative 3-WMRs and an object

and 1[m] at a constant speed in a anticlockwise direction. For the observation of  $\dot{\varphi}$ , we used a minimal order observer which is designed based on triple integrator model where the pole of observer is chosen to  $-50$ . Moreover in the experiment, the derived methods for considered robots are controlled by inputs regarded as signals for the rotational direction motors and PWM waves.

The desired trajectories and actual trajectories for cooperative 3-WMRs and an object are shown in Fig. 10, respectively. In this figure, it can be seen that the center of an object follows the desired trajectory through some tracking error exists due to uncertainties of parameters and effects of the dead reckoning. In Fig. 11, the

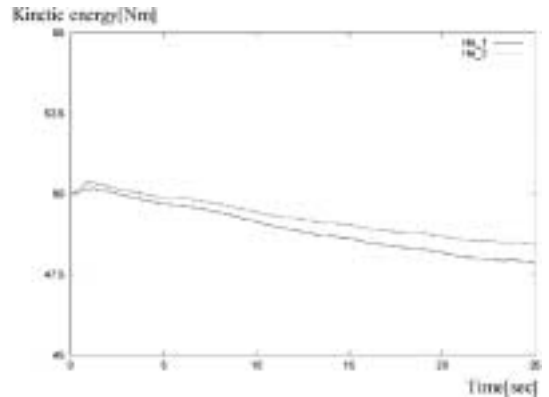


Fig. 12 Virtual energy for each augmented AGV system

tracking performance of angles for the desired signals is shown. It also shows good tracking performance. Finally, the changes of virtual energy are plotted in Fig. 12. It is seen from the figure that each virtual energy decreases slightly due to energy loss caused by incomplete cancellation of friction effects.

## 6. Conclusions

In this paper, we propose a new object-transportation control methodology for cooperative 3-WMRs convey a rigid object, and the proposed decentralized control algorithm is analyzed using an original PVFC algorithm. Especially, the closed-loop input/output systems for multiple robotic systems are passive with the environment

force as inputs, the system velocities as outputs, and the environment mechanical powers as supply rates as if it is similar to an original PVFC. The closed-loop systems for cooperative mobile robots are very effective in tracking a multiple of each desired velocity field and in counteracting the detrimental effect of environment disturbances when the disturbances are in the directions of the desired momentums of multiple robotic systems. Also, the performance will improve when the multiple robot systems are moving at high speed.

Moreover, the application of decentralized PVFC algorithm to tracing a circle as well as simulation and experimental results is presented in order to show effectiveness for the extended PVFC algorithm proposed in this paper.

### Acknowledgments

The work was supported by the National Research Laboratory Program of the Korean Ministry of Science and Technology (MOST).

### References

- Campion, G., Bastin, G. and D'Andrea-Novell, B., 1996, "Structural Properties and Classification of Kinematic and Dynamic Models of Wheeled Mobile Robots," *IEEE Trans. on Robotics and Automation*, Vol. 12, No. 1, pp. 47~62.
- D'Andrea-Novell, B., Bastin, G. and Campion, G., 1991, "Modeling and Control of Non Holonomic Wheeled Mobile Robots," *Proc. of IEEE ICRA*, pp. 1130~1135.
- Hashimoto, M., Oba, F. and Zenitani, S., 1995, "Object-Transportation Control by Multiple Wheeled Vehicle-Planar Cartesian Manipulator Systems," *Proc. of IEEE ICRA*, pp. 2267~2272.
- Kosuge, K. and Oosumi, T., 1996, "Decentralized Control of Multiple Robots Handling an Object," *Proceedings of IEEE IROS*, Vol. 1.
- Li, P. Y. and Horowitz, R., 2001a, "Passive Velocity Field Control (PVFC) Part I -Geometry and Robustness-," *IEEE Trans. on Automatic Control*, Vol. 46, No. 9, pp. 1346~1359.
- Li, P. Y. and Horowitz, R., 2001b, "Passive Velocity Field Control (PVFC) Part II -Application to Contour Following-," *IEEE Trans. on Automatic Control*, Vol. 46, No. 9, pp. 1360~1371.
- Park, T. J., Ahn, J. W. and Han, C. S., 2002, "A Path Generation Algorithm of an Automatic Guided Vehicle Using Sensor Scanning Method," *KSME International Journal*, Vol. 16, No. 2, pp. 137~146.
- Slotine, J. J. and Li, W., 1991, *Applied Non-linear Control*, Prentice-Hall Inc.
- Suh, J. H., Yamakita, M. and Kim, S. B., 2004, "Adaptive Desired Velocity Field Control for Cooperative Mobile Robotic Systems with Decentralized PVFC," *JSME International Journal, Series-C*, Vol. 47, No. 1, pp. 280~288.
- Yamakita, M., Suzuki, K., Zhen, X., Katayama, M. and Ito, K., 1998, "Cooperative Control for Multiple Manipulator Using an Extended Passive Velocity Field Control," *Trans. on IEE Japan*, Vol. 180-C, No. 1, pp. 21~28.
- Yamakita, M., Suh, J. H. and Hashiba, K., 2000, "Decentralized PVFC for Cooperative Mobile Robots," *Trans. on IEE Japan*, Vol. 120-C, No. 10, pp. 1485~1491.